

Multivariate hierarchical analysis of car crashes data considering a spatial network lattice

Andrea Gilardi, Jorge Mateu, Riccardo Borgoni and Robin Lovelace

November 26, 2020

Abstract

Road traffic casualties represent a hidden global epidemic, demanding evidence-based interventions. This paper demonstrates a network lattice approach for identifying road segments of particular concern, based on a case study of a major city (Leeds, UK), in which 5862 crashes of different severities were recorded over an eight-year period (2011-2018). We consider a family of Bayesian hierarchical models that include spatially structured and unstructured random effects, to capture the dependencies between the severity levels. Results highlight roads that are more prone to collisions, relative to estimated traffic volumes, in the North of the city. We analyse the Modifiable Areal Unit Problem (MAUP), proposing a novel procedure to investigate the presence of MAUP on a network lattice. We conclude that our methods enable a reliable estimation of road safety levels to help identify ‘hotspots’ on the road network and to inform effective local interventions.

Keywords: Bayesian hierarchical models; Car crashes data; MAUP; Multivariate modelling; Network lattice data; Spatial networks

1 Introduction

Road casualties have been described as a global epidemic [37, 46], representing the leading cause of death among young people worldwide. Car crashes and other types of collisions are responsible for more than 1 million deaths each year (1250000 in 2015, 17 deaths per 100000 people) [68]. In high income nations, such as the United Kingdom (UK), the roads are safer than the global average, but car crashes are still the cause of untold suffering. According to the statistics published by the UK’s Department for Transport (DfT) in the *Annual report on Road Casualties in Great Britain* [20], 153158 road traffic collisions resulting in casualties were recorded in 2019, 5% lower than 2018 and the lowest level since records began, in 1979. Nevertheless, the DfT estimates that approximately 33648 people were killed or seriously injured (KSI) in 2019¹, and while this number is slightly lower than in 2018, the decaying rate has been getting lower and lower starting from 2010. These figures are worrisome considering that car occupant fatality rates are particularly high in the 17-24 age band [20, p. 17].

¹The methodology for classifying the severity level of a car crash has been modified starting from 2016, adopting the injury-based systems called *CRASH* and *COPA* [13]. All police forces are gradually adopting these new reporting systems in England, and the Office for National Statistics (ONS) developed a logistic regression model to compare the severity levels between different years and classification systems. The data used in this paper have been adjusted using the procedures developed by ONS [20, pp. 38–41].

To tackle the flattening trend in the KSI rate over the past decades, a range of interventions are needed, and analytical approaches can help prioritise them. This paper presents a statistical model to identify street sections with anomalously high car crashes rates, and to support police responses and cost-effective investments in traffic calming measures [50].

Statistical models of road crashes have become more advanced over time. In the 1990s, models tended to consider only the discrete and heterogeneous nature of the data [43, 42, 58], omitting spatial characteristics. More recent statistical models of crash data include consideration of crash location in two-dimensional space, with three main advantages for road safety research [7]. First, consideration of space allows estimating appropriate measures of risk (such as expected counts, rates or probabilities) at different levels of resolution and the subsequent ranking of geographical areas to support local interventions. Second, spatial dependence can be a surrogate for unknown, potentially unmeasured (or unmeasurable) covariates; adjusting for geographic location can reduce model misspecification [21, 18]. Third, the spatial dimension can be used to take advantage of autocorrelation in the relevant variables, borrowing strength from neighbouring sites and improving model parameter estimation.

Road crash datasets, which are typically available on a single accident basis, can be spatially aggregated in two main ways: administrative zones (such as cantons, census wards, or regions) or street network features (either as contiguous segments or divided into corridors and intersections). In both cases, the spatial support is a lattice, i.e. a countable collection of geometrical units (polygons or lines, respectively), possibly supplemented by a neighbourhood structure. Several papers addressed the statistical modelling of crash frequencies at the areal level, based on available zoning systems in the study region (e.g. [45, 3, 47, 12]). The second approach has gained in popularity in recent years, with a number of papers analysing road crash events aggregated to the street level (e.g. [44, 2, 64]), as detailed in review papers [33, 57, 71]. In reference to street level data, we note that there has been a recent surge of research for spatial point patterns living on networks [55, 19, 5].

Both zone and network level approaches have advantages, notably computational requirements for the former and spatially disaggregated results for the latter. Given that computational resources are less of a constraint in the 2020s than they were in previous decades, and the fact that it is the nature of roads (not zones) that is responsible for crashes, we argue that road segments are the more appropriate aggregation units for the analysis of road crash data. Network analysis can be used to bring attention to specific segments, and, for these reasons, the models presented in the next sections were developed considering a network lattice.

Aggregation, e.g. number of crashes per road segment, enables comparison between different road segments. However, spatial aggregation also leads to a well-known problem in geographical analysis, the Modifiable Areal Unit Problem (MAUP), firstly described in [48]: the size of the spatial units impacts on the statistical analysis, influencing, and possibly biasing, modelling choices and results. Hence, conclusions drawn at one scale of spatial aggregation might not necessarily hold at another scale or be somehow different. The MAUP has been mainly ignored in the road safety literature and, as reported by [69] and [71, p. 21], it is mentioned only in a handful of recent papers [62, 1, 70, 15], which explore the impact of changing the areal zoning system (e.g. TAZ, block groups and census tracts) on parameter estimates, significance and hotspot detection. Only one early paper [60] could be found exploring the impacts of the MAUP on road crash data, albeit only in terms of summary statistics of aggregated counts. To assess the MAUP effect on network data modelling, we employed an algorithm to modify the structure of a road network, merging contiguous segments in the same corridor preserving the geometrical properties of the network [51]. Then, we compared the results obtained with the two different network configurations. To the best of our knowledge, this is the first attempt at exploring and estimating the

presence and the magnitude of MAUP in models that consider a network lattice.

Finally, we note that systems of collision classification present a multivariate nature [13, 30]. The occurrences of different severity degrees can be correlated to each other, and their spatial dynamics can be potentially interdependent. Hence, it is necessary to account for correlations between crashes counts at different levels of severity. We consider two types of accidents: *slight* and *severe*. The severe class is very sparse in the dataset at hand, hence modelling both types of accidents simultaneously allows to borrow strength from the existing correlations and improves estimates.

Following ideas introduced in [6], we consider a range of competing models, developed in a full hierarchical Bayesian paradigm. This approach allows one to encompass complex structures of spatial dependence in a quite natural way. Spatially structured random effects are defined using both Intrinsic Multivariate Conditional Auto-regressive (IMCAR) and Proper Multivariate Conditional Auto-regressive (PM-CAR) priors [8, 38, 41, 52]. We also propose to consider a generalisation of PMCAR models unexplored so far in the road safety literature, and firstly defined for polygonal lattice data in [23]. [33, 57, 71] review other examples of multivariate car crashes models on a network.

The case study is the metropolitan area of Leeds (population 800000) in North England. We accessed Ordnance Survey data on major roads (3661 segments, total length 450 km), creating a spatial network substantially larger than previous studies, many of which report findings on only a few roads, with [10] representing a notable exception albeit with a simpler spatial structure. We present results for an entire metropolitan area, approximating more closely the level at which road policing activities and investment in road safety interventions are prioritised. The scale of the case study presented several computational challenges, and, in terms of Bayesian parameter estimation, we used the computationally efficient Integrated Nested Laplace Approximation (INLA) approach instead of Markov chain Monte Carlo (MCMC) sampling [32, 56].

The rest of the paper is organised as follows. In Section 2, the data sources are described. In Section 3, the statistical methodology adopted in this paper is discussed in detail. In Section 4, the main results of the paper are presented whereas, model criticism and further model discussion, such as MAUP analysis, are provided in Section 5. Conclusions, in Section 6, end the paper.

2 Data

The datasets analysed in this paper came from several different sources and required a number of preprocessing steps before they could be made into a structure suitable for a statistical analysis. The study region was defined as the Middle Super Output Area (MSOA) zones within the local authority of Leeds. The City of Leeds was selected because it is a car-dependent city with a large network of major roads that approach the city centre (the city was dubbed the 'motorway city of the 70s') and would therefore be expected to be a place where road safety could be improved. Leeds is part of West Yorkshire and accounts for approximately 40% of all car crashes in the region. Origin-destination data from the 2011 UK Census were used to estimate traffic volumes, to provide an estimate of exposure, with traffic volumes used as the denominator in the statistical models presented in Section 3. Road network was obtained from Ordnance Survey, covering all major roads in Leeds.

We matched the network and the MSOAs using an overlay operation. Finally, we associated all car crashes that occurred in the city of Leeds from 2011 to 2018 with the nearest point on the road network, counting the occurrences in each street segment.

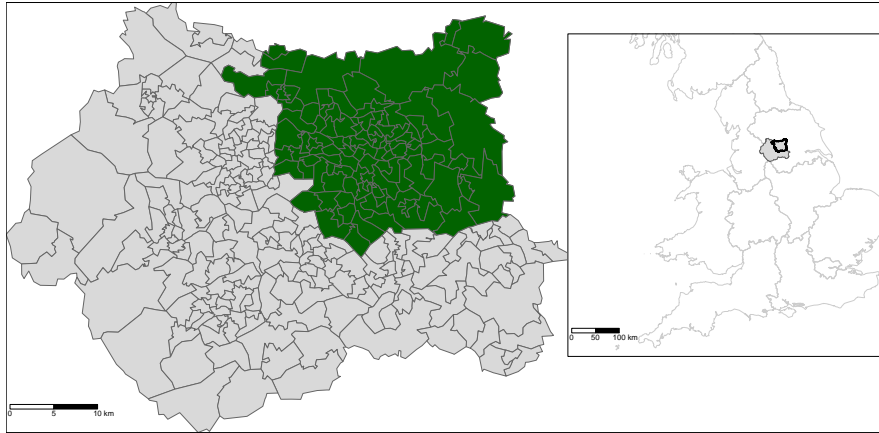


Figure 1: The grey polygons show the MSOAs in West-Yorkshire region, while the dark-green area highlights the city of Leeds. The inset map locates the position of the study-area with respect to England.

MSOA zones

There are 6791 MSOAs in England, 299 of which belong to the West-Yorkshire region. These were accessed from the [github-page](#)² of Propensity Cycle Tool [34], focussing, in particular, on the City of Leeds (107 areas). The MSOAs represent the starting point for all the following steps, and they are mapped in Figure 1 as grey polygons for the West-Yorkshire, and as dark-green polygons for the City of Leeds. The inset map is used to locate the study-area in the British territory.

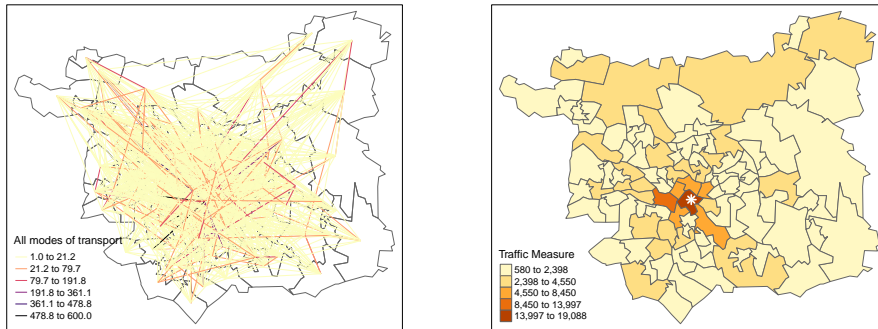
Traffic flow

The *traffic flow* data represent the *commuting journeys* from home to workplace using several modes of transport, such as train, bus, bike and motorcycle. The data were collected during the 2011 Census at the individual level, and then aggregated at the MSOA level. The UK Data Service shares the flow data through the *WICID* interface as cross-tables reporting the flows between all pairs of a predefined set of MSOAs [61]. We considered the commuting flows in the region of Leeds for all possible modes of transport. Figure 2a shows a random sample of 1000 *traffic flows*³ between the centroids of the MSOAs in Leeds, coloured according to the number of daily commuters.

Raw WICID data, however, ignore that people may travel to their workplace through several MSOAs. For this reason, we calculated a new traffic measure using the following procedure. Starting from the MSOAs, we defined a graph where the vertices are the centroids of each area, and the edges connect neighbouring areas. Then, we estimated the shortest path for all commuting journeys downloaded from WICID and assigned to each MSOA a value that is equal to the sum of all raw traffic measures going through the area. These values represent the new traffic measures and are displayed in Figure 2b. A similar approach was also adopted in [12], and we refer to the references therein for more details. The raw data flows and the MSOAs polygons were downloaded using the R package *pct* [34].

²Last access on 06/2020

³We downloaded 10536 traffic flows, which is slightly less than $107^2 = 11449$ since there are no commuters between certain MSOAs.



(a) Random sample of one thousand Origin-Destination data representing the daily flows between MSOAs in Leeds.

(b) Estimates of the new traffic measure. The white star represents Leeds City Centre.

Figure 2: Raw and modified traffic flows in the area of Leeds. The map on the right highlights several contiguous MSOAs that correspond to the arterial thoroughfares that are used to reach the City Centre.

Road network

The *road network* was built using data downloaded from Ordnance Survey (OS)⁴, an agency that provides digital maps and other services for location-based products [49]. We downloaded the *Vector OpenMap Local* data for the *SE* region⁵, selected the *Roads* and *Tunnels* layers, and filtered the streets that belong to the City of Leeds. Ordnance Survey represents all the streets of a road network as the union of a finite set of segments, and it includes additional fields such as the road name or the street type. These segments represent the elementary units for the statistical analysis described in Section 3.

The road network downloaded from OS is composed of approximately 50000 segments. The OS network was simplified using the following procedure. We first selected only the major roads, such as the *motorways*, *primary roads* and *A roads*. They represent less than 10% of the total road network, but more than 50% of all car crashes registered during 2011-2018 occurred in their proximity. The output of this procedure is a road network composed by a big cluster of connected streets, displayed in Figure 4a, and several small isolated groups of road segments (which are also called *islands*), created by the exclusion of their links to the other roads.

These small clusters can be problematic from a modelling perspective since they produce a not-fully-connected network (see [28, 22] and the properties of ICAR and MICAR distributions explained in Section 3), so we implemented an algorithm to further simplify the road network and remove them. This algorithm is based on the dual representation of a road network as a geographical entity, composed by points and lines, and a graph object, with nodes and edges [53, 40, 25]. More precisely, we created a graph whose vertices correspond to the street segments of the road network, and we defined an edge for each pair of spatial units sharing a point at their boundaries. This graph uniquely determines a (sparse) adjacency matrix amongst the spatial units (i.e. the road segments), that summarises the graph dimension of the road network. We sketched a toy example in Figure 3, representing the idea behind

⁴Last access on 21-05-2020

⁵The United Kingdom has been divided into several squares of approximately 100km^2 . The SE region is an area centred around Leeds. See <https://www.ordnancesurvey.co.uk/business-government/tools-support/vectormap-district-support> for a list of maps displaying all OS areas.

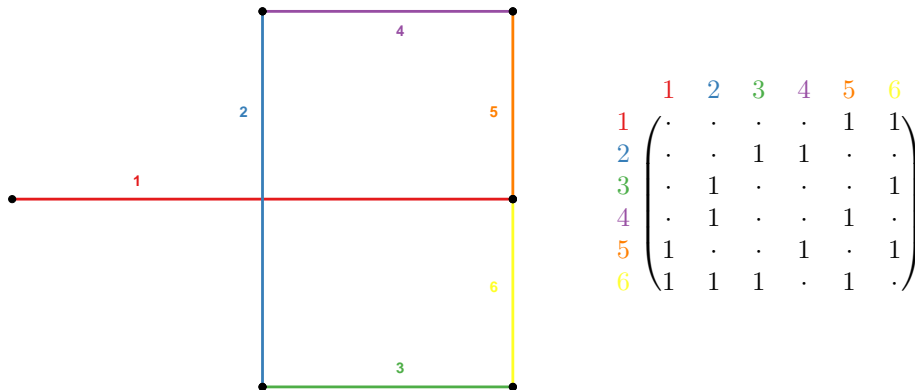


Figure 3: Graphical example showing the dual nature of a road network. *Left*: map showing the geographical dimension. Each segment is coloured and labelled using a different ID and colour respectively. *Right*: adjacency matrix of the graph associated with the road network. Each vertex corresponds to a segment whereas an edge connects two vertices if they share one boundary point. For example, segments 1 and 2 are not neighbours since they do not share any point at the boundaries, even if they intersect each other. This situation may occur at bridges or overpasses.

the dual representation of a road network and the definition of the adjacency matrix.

Then, starting from the graph and the adjacency matrix, we calculated its *components*⁶, and we excluded all small clusters of road segments that did not belong to the biggest *component*. It should be stressed that this procedure creates a fully connected network, which has relevant consequences on the rank-deficiency problem of the ICAR models described in Section 3. In the end, the road network is composed of approximately 3600 units, and it is shown in Figure 4a, where the segments are coloured according to their road types. Moreover, since the street network and the MSOAs are spatially misaligned, they were matched using an overlay operation: each road segment was assigned to the MSOA that intersects the largest fraction of the segment. This procedure allows us to assign a traffic estimate to each road segment, which will be used as an exposure parameter in the statistical models considered below.

Car crashes data

We analysed all *car crashes* that occurred between the 1st of January 2011 and the 31st of December 2018 in the MSOAs pertaining to the City of Leeds, which involved personal injuries, occurred on public roads and became known to the Police forces within thirty days of the occurrence. The data were downloaded from the UK's official road traffic casualty database, called *STATS19*, using the homonym R package [35]. We excluded all car crashes that occurred farther than ten meters from the closest segment in the simplified road network since they are probably related to other streets. *STATS19* data also report the severity level of each casualty using one of three possible

⁶A graph is said to be *connected* if there exist a sequence of edges going from each vertex to every other vertex. The *components* of a graph are sub-graphs formed by all connected vertices [31].

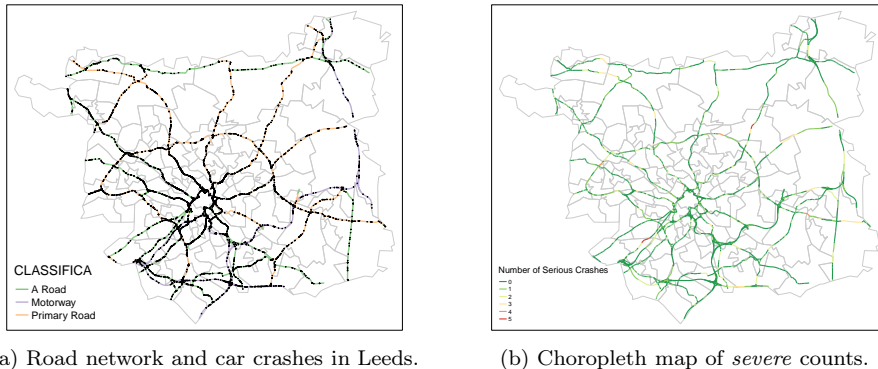


Figure 4: The map on the left represents the road network in Leeds. Each segment is coloured according to its OS classification. The black dots represent the car crashes. On the right, we report a choropleth map displaying *severe* car crashes counts.

categories: *fatal*, *serious* or *slight*⁷ We harmonised the severity levels for different years and police forces using the CRASH methodology [20, 13], and we decided to aggregate *serious* and *fatal* levels since *fatal* crashes represent approximately 1% of the total number of car accidents. Henceforth, we will refer to *serious* or *fatal* crashes as *severe* accidents. The final sample is composed of 5862 events, and they are reported as black dots in Figure 4a. Then, we projected all crashes to the nearest point on the road network, and we counted the number of *slight* or *severe* occurrences on all street segments. We decided to ignore the temporal dimension since *severe* crashes counts present an extreme sparsity, with more than 80% of zero counts during 2011-2018. Moreover, 40% of all segments registered no car crashes during the study period, while another 40% reported two or more crashes. These numbers highlight a common temporal trend between the eight years, and we refer the interested reader to the supplementary material for a space-time representation. The map in Figure 4b shows the spatial distribution of *severe* crashes counts.

3 Statistical methodology

We first focus on the definition of a three-level hierarchical model structure, which is shared among all the alternative specifications considered below. Then, we introduce two baseline models that serve as benchmarks and starting points for the other specifications. Thereafter, five different extensions to the baseline models are introduced. Finally, some techniques used for model comparison are discussed. The common theme behind all the seven alternatives is the presence of spatially structured and unstructured multivariate random effects.

Let Y_{ij} , $i = 1, \dots, n$, represent the number of car crashes that occurred in the i -th road segment with severity level j , $j = 1, \dots, J$. In this paper we consider two possible severity levels, a car crash being either *severe*, $j = 1$, or *slight*, $j = 2$.

⁷An accident is classified as *fatal* if it involved a human casualty whose injuries caused his death less than thirty days after the accident; *severe* if at least one person was hospitalised after the accident or recorded a particular type of injury (like concussions or severe cuts), and *slight* in all the other cases.

In the first stage of the hierarchy, we assume that

$$Y_{ij}|\lambda_{ij} \sim \text{Poisson}(E_i\lambda_{ij}),$$

where E_i is an exposure parameter and λ_{ij} represents the car crashes rate in the i th road segment for severity level j . At the second stage of the hierarchical model, a log-linear structure of λ_{ij} is specified. We assume that

$$\log(\lambda_{ij}) = \beta_{0j} + \sum_{m=1}^M \beta_{mj} X_{ijm} + \theta_{ij} + \phi_{ij},$$

where β_{0j} represents a severity-specific intercept, $\{\beta_{mj}\}_{m=1}^M$ is a set of coefficients, $(X_{ij1}, \dots, X_{ijM})$ is a collection of M covariates, ϕ_{ij} is a spatially structured random effect and θ_{ij} represents a normally distributed error component. The third stage that completes the hierarchical model is the specification of prior and hyperprior distributions. We assigned a vague $N(0, 1000)$ prior to β_{mj} , $m = 0, \dots, M$. The two random effects, namely θ_{ij} and ϕ_{ij} , represent the structured and unstructured spatial components and are defined differently in different models as discussed below. Hereafter, we follow the notation used in [41, Ch 4, 6 and 8].

3.1 Baseline models: independent spatial and unstructured effects

The two baseline models are defined considering multivariate spatial and unstructured random effects with independent components. More precisely, a bivariate Gaussian prior with independent components is assigned to $(\theta_{i1}, \theta_{i2})$ for both baseline models:

$$(\theta_{i1}, \theta_{i2}) \sim N_2\left(\mathbf{0}, \begin{bmatrix} \sigma_{\theta_1}^2 & 0 \\ 0 & \sigma_{\theta_2}^2 \end{bmatrix}\right), \quad i = 1, \dots, n. \quad (1)$$

We assigned a Gamma hyperprior with parameters 1 (shape) and 0.00005 (inverse scale) to the inverse of $\sigma_{\theta_1}^2$ and $\sigma_{\theta_2}^2$, i.e. the precisions.

The spatially structured term in the first baseline model was defined using an *Independent Intrinsic Multivariate Conditional Auto-regressive* (IIMCAR) prior, whereas, for the second model, we adopted an *Independent Proper Multivariate Conditional Auto-regressive* (IPMCAR) prior. The IIMCAR and IPMCAR distributions are briefly introduced hereafter, starting from their classical univariate counterparts, namely the ICAR and PCAR distributions.

Univariate spatial random effects are traditionally modelled using a prior that belongs to the family of *Conditional Auto-regressive* (CAR) distributions [8]. Given a random vector $\phi = (\phi_1, \dots, \phi_n)$, the *Intrinsic Conditional Auto-Regressive* (ICAR) distribution, which is a particular case of the CAR family, is usually defined through a set of conditional distributions [9]:

$$\phi_i|\{\phi_{i'}, i' \in \partial_i\}; \sigma^2 \sim N\left(m_i^{-1} \sum_{i' \in \partial_i} \phi_{i'}, \frac{\sigma^2}{m_i}\right), \quad i = 1, \dots, n, \quad (2)$$

where ∂_i and m_i denote, respectively, the indices and the cardinality of the set of neighbours for spatial unit i . These quantities are defined through a sparse binary symmetric neighbourhood matrix \mathbf{W} with dimensions $n \times n$, that summarises the spatial relationships in the region of study. We built it taking advantage of the dual representation of a road network as a spatial and a graph object (see the *Road Network* in Section 2). More precisely, \mathbf{W} is the adjacency matrix of a graph whose vertices correspond to the street segments of the road network and the edges identify a shared point at the boundaries of two spatial units. This procedure defines a *First Order*

neighbourhood matrix. *Second* and *Third Order* neighbourhood matrices are defined iteratively in the same way.

It is possible to prove that the prior defined by (2) suffers from rank-deficiency problems, that are usually fixed by imposing a set of sum-to-zero constraints on the vector ϕ , one for each *component* in the graph of the road network [28]. In this paper, we deal with a fully connected road network (see the pre-processing procedures detailed in Section 2), so we always had to fix only one set of constraints.

The *Proper Conditional Auto-Regressive* (PCAR) distribution is another member of the CAR family and it is usually defined as follows:

$$\phi_i | \{\phi_{i'}, i' \in \partial_i\}; \sigma^2, \rho \sim N \left(\rho \left(m_i^{-1} \sum_{i' \in \partial_i} \phi_{i'} \right), \frac{\sigma^2}{m_i} \right), \quad i = 1, \dots, n, \quad (3)$$

where ∂_i and m_i are defined as for the ICAR distribution and ρ is a parameter controlling the strength of spatial dependence, usually called *spatial autoregression coefficient* [18]. It is possible to prove that the joint distribution defined by (3) is proper if $|\rho| < 1$, hence there is no need to set any sum-to-zero constraint in this case. The ICAR prior can be seen as a limit case of the PCAR distribution with $\rho \rightarrow 1$, analogously to the relationship between Auto-Regressive and Random-Walk models in time series models [11].

The family of *Multivariate Conditional Auto-regressive* (MCAR) distributions was firstly introduced by [38], extending the ideas of [8] to the multivariate case. Given a random matrix $\Phi = (\phi_{ij})$, which is defined for $i = 1, \dots, n$ units and $j = 1, \dots, J$ levels, the *Intrinsic Multivariate Conditional Auto-regressive* (IMCAR) distribution is a particular case of the MCAR family, defined through a set of multivariate conditional distributions [41]:

$$\Phi_i | \text{vec}(\Phi_{-i}); \Omega \sim N_J \left(m_i^{-1} \sum_{i' \in \partial_i} \Phi_{i'}^T; m_i^{-1} \Omega^{-1} \right). \quad (4)$$

The terms Φ_i and Φ_{-i} denote, respectively, the i th row of Φ and the matrix obtained by excluding the i th row from Φ . The vec operator is used for row-binding the columns of a matrix, meaning that $\text{vec}(\Phi_{-i}) = (\Phi_{-i,1}^T, \dots, \Phi_{-i,J}^T)^T$. The elements m_i and ∂_i are defined as before, through the adjacency matrix \mathbf{W} of the graph associated to the road network, and they represent the spatial dimension of the IMCAR distribution. The $J \times J$ precision matrix Ω is used to model the associations between pairs of levels in the same road segment i , and it acts as a multivariate extension of the parameter σ^2 in (2).

This distribution suffers from the same rank-deficiency problems as its univariate counterpart, which are usually solved by imposing appropriate sum-to-zero constraints. The number of restrictions is equal to the number of *components* in the graph of the road network times the number of levels in the multivariate setting. The pre-processing operations that we performed on the network data (see Section 2) imply that we always have to set only J sum-to-zero constraints.

The IIMCAR distribution is a particular case of (4), which is obtained by setting $\Omega^{-1} = \text{diag}(\sigma_{\phi_1}^2, \dots, \sigma_{\phi_J}^2)$. More precisely, if we assume $J = 2$ as we do in this paper, then IIMCAR is defined by the following set of multivariate conditional distributions:

$$\Phi_i | \text{vec}(\Phi_{-i}); \sigma_{\phi_1}^2, \sigma_{\phi_2}^2 \sim N_2 \left(m_i^{-1} \sum_{i' \in \partial_i} \Phi_{i'}^T; m_i^{-1} \begin{bmatrix} \sigma_{\phi_1}^2 & 0 \\ 0 & \sigma_{\phi_2}^2 \end{bmatrix} \right). \quad (5)$$

In equation (5) we are assuming independence between the 2 levels, and this implies that the IIMCAR distribution is equivalent to two independent ICAR distributions, one for each level.

Analogously to the univariate case, the *Proper Multivariate Conditional Autoregressive* (PMCAR) distribution is a particular case of the MCAR family characterised by the following set of multivariate conditional distributions:

$$\Phi_i | \text{vec}(\Phi_{-i}); \rho, \Omega \sim N_J \left(m_i^{-1} \rho \sum_{i' \in \partial_i} \Phi_{i'}^T; m_i^{-1} \Omega^{-1} \right). \quad (6)$$

The strength of the spatial dependence is controlled by ρ (as for the univariate PCAR distribution) and all the other parameters are defined as before. It can be proved that the joint distribution defined by equation (6) is proper if $|\rho| < 1$, although we restricted ourselves to $\rho \in (0, 1)$ to avoid some counter-intuitive behaviour of the PMCAR distribution [63, 44].

The IPMCAR distribution is defined as a particular case of equation (6) with $\Omega^{-1} = \text{diag}(\sigma_{\phi_1}^2, \dots, \sigma_{\phi_J}^2)$. More precisely, if we assume $J = 2$, then IPMCAR is defined through the following set of multivariate conditional distribution:

$$\Phi_i | \text{vec}(\Phi_{-i}); \rho, \sigma_{\phi_1}^2, \sigma_{\phi_2}^2 \sim N_2 \left(m_i^{-1} \rho \sum_{i' \in \partial_i} \Phi_{i'}^T; m_i^{-1} \begin{bmatrix} \sigma_{\phi_1}^2 & 0 \\ 0 & \sigma_{\phi_2}^2 \end{bmatrix} \right). \quad (7)$$

For the same reasoning as in equation (5), the IPMCAR distribution is equivalent to J independent PCAR distributions.

Now we can characterise the random effects for the two baseline models. The first model was defined by considering unstructured random effects with a bivariate independent Gaussian prior (1), and spatial random effects with an IIMCAR prior (5). The second one was defined analogously to the first baseline model, but assuming an IPMCAR distribution for the spatial random effects (7). These models assume independence between the two levels both in the spatial and unstructured components, so they were used as benchmarks. In the next sections, we will also refer to the two baseline models using, respectively, the codes (A) and (B). We assigned an improper prior to σ_1^2 and σ_2^2 , the variances in Ω , defined on \mathbb{R}^+ , and a Uniform(0, 1) prior to ρ .

Hereafter we introduce three increasingly complex sets of extensions that generalise the baseline models. The first one is characterised by the removal of the independence assumption from the spatially structured random effects, whereas, in the second set of extensions, we also relax the independence assumption from the unstructured random effects. The third and last set of extensions is characterised by a generalisation of PMCAR distribution that introduces a separate spatial autoregression coefficient, ρ_j , for each level in Φ .

3.2 Model extensions

First set of extensions

Starting from the baselines, we defined two new models replacing the IIMCAR and IPMCAR priors with their non-independent multivariate counterparts, the generic IMCAR and PMCAR defined above. If we assume $J = 2$, then the variance-covariance matrix Ω^{-1} in (4) and (6) can be written as

$$\Omega^{-1} = \begin{bmatrix} \sigma_{\phi_1}^2 & \rho_{\phi} \sigma_{\phi_1} \sigma_{\phi_2} \\ \rho_{\phi} \sigma_{\phi_1} \sigma_{\phi_2} & \sigma_{\phi_2}^2 \end{bmatrix},$$

where σ_1^2 and σ_2^2 represent the conditional variances and ρ_{ϕ} represents the correlation coefficient between the two levels in the same spatial unit. These models represent a generalisation of the baselines since we are now taking into account the correlations between different levels in the same road segment. We will also refer to them using,

respectively, the codes (C) and (D). Following [52], we assigned a Wishart hyperprior to Ω^{-1} with parameters 2 and \mathbf{I}_2 , i.e. the identity matrix of size two. The prior distributions on the unstructured random effects were left unchanged with respect to the baselines.

Second set of extensions

In these models, the independence assumption of the spatially unstructured random effects is removed. More precisely, assuming $J = 2$, we assign a generic bivariate Gaussian prior to the unstructured random effects:

$$(\theta_{i1}, \theta_{i2}) \sim N_2 \left(\mathbf{0}, \begin{bmatrix} \sigma_{\theta_1}^2 & \rho_{\theta} \sigma_{\theta_1} \sigma_{\theta_2} \\ \rho_{\theta} \sigma_{\theta_1} \sigma_{\theta_2} & \sigma_{\theta_2}^2 \end{bmatrix} \right).$$

Parameters $\sigma_{\theta_1}^2$ and $\sigma_{\theta_2}^2$ represent the marginal variances of the unstructured random error, whereas ρ_{θ} represents their correlation. These models will also be identified using the codes (E) and (F). We assigned a Wishart hyperprior to the variance-covariance matrix with parameters 2 and \mathbf{I}_2 .

Third set of extensions

It is possible to prove (e.g. [38]) that the set of conditional normal random variables defined by equation (6) induce a multivariate joint distribution for $\text{vec}(\Phi)$ that can be written as

$$\text{vec}(\Phi) \sim N_{nJ}(\mathbf{0}, [\Omega \otimes (\mathbf{D} - \rho\mathbf{W})]^{-1}) \quad (8)$$

where \mathbf{D} is a $n \times n$ diagonal matrix whose elements d_{ii} are equal to m_i , the number of neighbours for spatial unit i and \otimes denotes the Kronecker product. The precision matrix in Equation (8) is given by the Kronecker product of two quantities: Ω , that models the variability between the J levels in the same road segment i , and $(\mathbf{D} - \rho\mathbf{W})$, that models the spatial variability between different road segments for the same level j .

In the third set of extensions, following [23], we generalised the PMCAR distribution, defining a model which introduces a different spatial autocorrelation coefficient ρ_j for each level in Φ . More precisely, we set

$$\text{vec}(\Phi) \sim N_{nJ} \left(\mathbf{0}, \left[\text{bdiag}(\mathbf{R}_1, \dots, \mathbf{R}_J) (\Omega \otimes \mathbf{I}_n) \text{bdiag}(\mathbf{R}_1, \dots, \mathbf{R}_J)^T \right]^{-1} \right) \quad (9)$$

where $\mathbf{R}_j, j = 1, \dots, J$ is the Cholesky decomposition of $\mathbf{D} - \rho_j\mathbf{W}$, i.e. $\mathbf{R}_j\mathbf{R}_j^T = \mathbf{D} - \rho_j\mathbf{W}$, and $\text{bdiag}(\mathbf{R}_1, \dots, \mathbf{R}_J)$ denotes a block-diagonal matrix with elements $\mathbf{R}_1, \dots, \mathbf{R}_J$ and dimension $nJ \times nJ$.

For example, assuming $J = 2$, the precision matrix in equation (9) can be written as

$$\begin{bmatrix} \mathbf{R}_1 & 0 \\ 0 & \mathbf{R}_2 \end{bmatrix} (\Omega \otimes \mathbf{I}_2) \begin{bmatrix} \mathbf{R}_1 & 0 \\ 0 & \mathbf{R}_2 \end{bmatrix}^T.$$

It is possible to prove that the joint distribution defined by equation (9) is proper if $|\rho_j| < 1 \forall j$ and, following the same ideas as before, we assigned a Wishart hyperprior to Ω^{-1} with parameters 2 and \mathbf{I}_2 , and a Uniform(0, 1) prior to ρ_1 and ρ_2 . We will refer to this last model using the code (G).

We summarised in Table 1 the prior distributions adopted for the random effects in the two baselines and their extensions. We also included the IDs that will be used to identify each model in subsequent Tables and Sections.

ID	Model	Unstructured Effect	Spatial effect
(A)	Baseline 1	Independent Gaussian	Independent IMCAR
(B)	Baseline 2	Independent Gaussian	Independent PMCAR
(C)	Extension 1 - Model 1	Independent Gaussian	IMCAR
(D)	Extension 1 - Model 2	Independent Gaussian	PMCAR
(E)	Extension 2 - Model 1	Correlated Gaussian	IMCAR
(F)	Extension 2 - Model 2	Correlated Gaussian	PMCAR
(G)	Extension 3	Correlated Gaussian	PMCAR - Multiple ρ

Table 1: Summary of the prior distributions assigned to the random effects in the models introduced in Section 3.

3.3 Model comparison

The models proposed in the previous paragraphs were compared using Deviance Information Criterion (DIC) [59] and Watanabe–Akaike Information Criterion (wAIC) [24, 67]. These criteria represent a measure for the adequacy of a model, penalised by the number of effective parameters. In both cases, the lower is the value of the index, the better is the fitting of the model.

4 Results

We estimated the models previously described using the software *INLA* [32, 56, 26], interfaced through the homonymous R package [54]. We used the *Simplified Laplace* strategy for approximating the posterior marginals and the *Central Composite Design* strategy for determining the integration points. The code behind the definition of multivariate ICAR and PCAR random effects is defined in the package *INLAMSM* [52], and we wrote the functions used to estimate the spatial random effects in model (G). It took approximately 30 - 45 minutes to estimate each model using a virtual machine with an Intel Xeon E5-2690 v3 processor, six cores, and 32GB of RAM.

Fixed effects

The models listed in Table 1 share a common structure for the fixed effect component, with a severity-specific intercept and a set of covariates, representing some characteristics of the road segments. We considered two severity-specific covariates: the road type (either *Motorway*, *Primary Road* or *A Road*, according to OS definition), and the edge betweenness centrality measure, which reflects the number of shortest paths traversing each segment [31]. It can be considered as a proxy for the average vehicle miles traveled (VMT) [14]. Following the suggestions in [64], the exposure parameter, E_i , is given by the product of two quantities: the segment’s length and the estimate of traffic flow (see Section 2).

Table 2 shows the posterior means and standard deviations for the fixed effects. We first notice that the estimates are stable among the models. The intercept for severe car crashes, β_{01} , is found slightly smaller than β_{02} . This is not surprising since severe accidents are rarer than the slight ones. The coefficients of edge betweenness centrality measures are found close to zero for all models, and their 95% credible interval (not reported in the table) always include the value zero. Road type parameters represent relative differences with respect to the reference category (i.e. *A Roads*), hence *Motorways* are found less prone to severe and slight car crashes than *A roads*. A similar finding was also reported by [12] for UK data. An analogous interpretation

applies to *Primary Roads*.

Random effects

The posterior means and standard deviations for all hyperparameters are reported in Table 3, which reflects the models' nested structure, also summarised in Table 1. We started from two baselines, (A) and (B), with independent random effects, and generalised them until model (G), that presents multiple spatial autocorrelations between the severity levels.

Models from (A) to (D), which assume independent unstructured random effects, exhibit a degenerate posterior distribution of $\sigma_{\theta_1}^2$, i.e. the variance of severe random component, and this is possibly due to the severe car crashes sparseness. This problem gets mitigated once the correlation parameter between the two severity levels is included in the model, suggesting that the estimation procedure benefits from the inclusion of a multivariate structure that allows borrowing strength from less rare events.

The estimates of $\sigma_{\theta_2}^2$ and ρ_θ are stable among the models, and the correlation parameter is estimated as high as 0.40, suggesting a positive and mildly strong relationship between the two random components.

The posterior means for hyperparameters ρ in models (B), (D), (F) and (G), are always very close to one, which is not uncommon for this type of models [17]. In particular, the spatial autocorrelation coefficient of model (G) is found higher for slight car crashes than its severe counterpart, indicating a greater spatial homogeneity, something that can also be related with the sparse nature of severe car crashes.

The estimates of the posterior distributions for the two conditional variances, $\sigma_{\phi_1}^2$ and $\sigma_{\phi_2}^2$, are found less stable compared to the unstructured errors. The credible intervals of the two hyperparameters overlap in all models, indicating a similar spatial structure between the two kinds of severities. The posterior mean of ρ_ϕ , the correlation coefficient between the two severity levels, is found approximately equal to 0.85, indicating a strong multivariate nature for the spatial random component.

These results suggest that car crash data have a complex latent structure being the severity levels strongly correlated, and the spatially structured and unstructured effects statistically relevant.

Model comparisons

We compared the models listed in Table 1 using DIC and wAIC criteria. The results are reported in Table 4.

PMCAR models (i.e. (B), (D) and (F)) are found to perform always better than their Intrinsic counterparts in terms of goodness of fit. They are somewhat unexplored in the road safety literature on spatial networks, [44] being the only paper we found that analyse the importance of a spatial autocorrelation parameter. However, our results suggest that PCAR distribution and its generalisations should deserve more attention.

Moving from (A) to (G) the model performance improves, indicating one more time the benefits of considering a correlated multivariate structure for the spatial and the unstructured components. In particular, model (G), which includes a specific spatial autocorrelation parameter for each severity level, is the best one according to both criteria; hence, hereafter, we focus on this model.

Car crashes rate

Figure 5 displays the posterior means of car accident rates, λ_{ij} , estimated using model (G) both for severe and slight crashes. The colours of the road segments were generated by dividing the predicted values of each severity level into ten classes based on quantiles

ID	Severe Crashes				Slight Crashes			
	β_{01}	Betweenness	Motorways	Primary Roads	β_{02}	Betweenness	Motorways	Primary Roads
(A)	-14.325 (0.090)	0.018 (0.056)	-0.828 (0.173)	0.330 (0.146)	-12.834 (0.061)	-0.057 (0.034)	-0.112 (0.116)	0.601 (0.102)
(B)	-14.430 (0.156)	0.003 (0.056)	-0.825 (0.179)	0.344 (0.146)	-12.856 (0.134)	-0.065 (0.034)	-0.143 (0.119)	0.580 (0.102)
(C)	-14.342 (0.090)	-0.065 (0.056)	-0.746 (0.179)	0.378 (0.147)	-12.816 (0.061)	-0.084 (0.034)	-0.104 (0.119)	0.578 (0.104)
(D)	-14.463 (0.116)	-0.098 (0.050)	-0.738 (0.174)	0.487 (0.127)	-12.820 (0.098)	-0.069 (0.034)	-0.187 (0.122)	0.549 (0.101)
(E)	-14.375 (0.089)	-0.013 (0.055)	-0.787 (0.176)	0.415 (0.142)	-12.816 (0.061)	-0.061 (0.034)	-0.120 (0.116)	0.584 (0.102)
(F)	-14.460 (0.133)	-0.058 (0.052)	-0.767 (0.175)	0.458 (0.133)	-12.833 (0.119)	-0.066 (0.034)	-0.163 (0.120)	0.556 (0.102)
(G)	-14.475 (0.126)	-0.063 (0.052)	-0.772 (0.175)	0.469 (0.131)	-12.832 (0.118)	-0.068 (0.034)	-0.164 (0.120)	0.558 (0.102)

Table 2: Estimates for the posterior means and standard deviations, in round brackets, of the fixed effects included in the models described in Table 1.

14

ID	$\sigma_{\theta_1}^2$	$\sigma_{\theta_2}^2$	ρ_{θ}	ρ	$\sigma_{\phi_1}^2$	$\sigma_{\phi_2}^2$	ρ_{θ}	
(A)	0.0001 (0.0001)	0.782 (0.038)			0.148 (0.021)	0.131 (0.015)		
(B)	0.0001 (0.0001)	0.670 (0.049)		0.998 (0.0006)	0.268 (0.041)	0.253 (0.038)		
(C)	0.0001 (0.0001)	0.597 (0.047)			0.315 (0.039)	0.270 (0.031)	0.905 (0.019)	
(D)	0.0001 (0.0001)	0.358 (0.055)		0.987 (0.004)	0.752 (0.105)	0.725 (0.102)	0.904 (0.019)	
(E)	0.573 (0.083)	0.757 (0.047)	0.414 (0.008)		0.141 (0.024)	0.147 (0.019)	0.804 (0.041)	
(F)	0.462 (0.077)	0.632 (0.048)	0.402 (0.013)	0.997 (0.001)	0.291 (0.042)	0.300 (0.035)	0.838 (0.035)	
(G)	0.440 (0.084)	0.633 (0.049)	0.402 (0.013)	0.995 (0.002)	0.997 (0.001)	0.341 (0.066)	0.302 (0.042)	0.842 (0.031)

Table 3: Estimates for the posterior means and standard deviations, in round brackets, of hyperparameters included in the models described in Table 1.

ID	DIC	wAIC
(A)	14472.38	14479.97
(B)	14429.88	14445.44
(C)	14271.16	14296.64
(D)	14160.68	14173.21
(E)	14136.85	14118.19
(F)	14114.91	14094.39
(G)	14113.36	14093.90

Table 4: Estimates of DIC and wAIC values for the models described in Section 3.

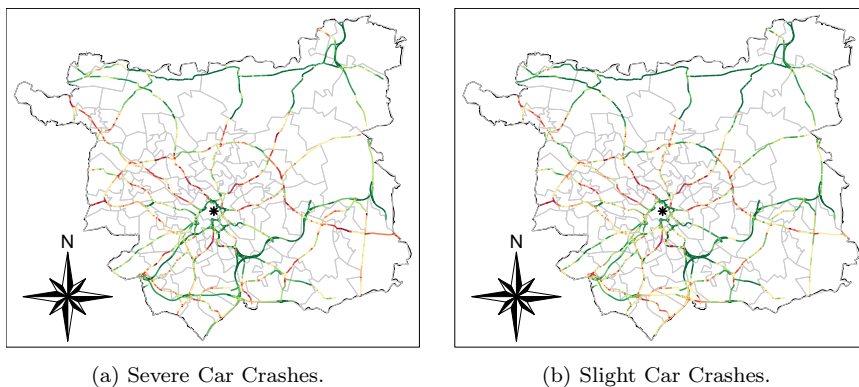


Figure 5: Maps representing the posterior means for severe and slight car crashes rates, estimated using model (G). The colours go from red (higher quantiles) to green (lower quantiles). The black star represents Leeds City Centre.

ranging from red (highest quantile) to dark green (lowest quantiles). The black star in the middle of the map denotes Leeds City Centre. The two maps show similar patterns, but some roads in the southern part of the city (especially M621) look more prone to severe car crashes. The city of Leeds appeared to be divided into several areas. The northern and eastern part of the city are associated with lower car accident rates compared to other suburbs. The areas located in the north, north-west and south-east of the city centre seem to be associated with the highest levels of car crashes rates, especially severe ones. Finally, we note that the roads closer to the city centre are the safest part of the city network.

5 Model criticism and sensitivity analysis

DIC and wAIC criteria were never intended to be absolute measures of model fit, and they cannot be used for *Model Criticism*. Hence, we tested the adequacy of model (G) using two strategies.

		Predicted Counts	
		Zero	One or more
Actual Counts	Zero	A	B
	One or more	C	D

Sensitivity	$= \frac{A}{A+B}$
Specificity	$= \frac{D}{C+D}$
Accuracy	$= \frac{A+D}{A+B+C+D}$
Balanced Accuracy	$= \frac{1}{2} \left(\frac{A}{A+B} + \frac{D}{C+D} \right)$

Table 5: Left: Confusion matrix showing the observed and predicted counts, binned in two classes. Right: Definition of accuracy measures.

5.1 First strategy for criticism

The classical criterion for criticism of a Bayesian hierarchical model is the Probability Integral Transform [39, 27], typically adjusted in case of a discrete response variable (such as car crashes counts) using a continuity correction. Unfortunately, these adjustments do not seem to work appropriately when modelling sparse count data, such as severe crashes, since the correction is not adequate. We refer the interested reader to the supplementary material for more details.

Therefore, hereafter, we followed a different strategy. We binned the observed and predicted counts into two classes: *Zero* and *One or more* car crashes⁸. Then, we built a confusion matrix and evaluated the model performance via some accuracy measures that are summarised in Table 5. A similar correction for sparse count data was also presented in [36].

The *accuracy* measure, usually adopted for evaluating the predictive performance of a model, is typically biased and overly-optimistic in case of unbalanced classes (such as *Zero* and *One or more* severe car crashes per road segment), since, even in the worst case, it is as high as the percentage of observations in the more frequent class [16]. The *balanced accuracy*, firstly introduced by [16], is defined as the average of Sensitivity and Specificity, and it overcomes this drawback since it represents an average between the predictive performances on each class.

The output of a Bayesian hierarchical model is an estimate of the posterior distribution of predicted values, while the procedure reported in the previous paragraph can only be applied to binary data. For this reason, we simulated n Poisson random variables (one for each road segment) with mean equal to the mean of each posterior distribution. Then, we binned the observed and sampled counts into two classes, i.e. *Zero* and *One or more* car crashes, and we compared the two values, obtaining a single estimate of balanced accuracy. Its distribution was finally approximated by repeating this procedure $N = 5000$ times.

Moreover, we calculated several quantiles of the posterior distribution of each predicted value, and we run the same steps as in the previous paragraph sampling from a Poisson distribution with mean equal to each of those quantiles. Lastly, being severe and slight car crashes potentially quite different processes, this algorithm was applied independently for the two severity levels. We reported in the supplementary material the pseudo-code for this procedure, whereas results are displayed in Figure 6a (severe crashes) and Figure 6b (slight crashes). In both cases, the red curve represents the distribution of balance accuracy obtained by a binary classification based on the posterior means, whereas the other curves represent the same distribution obtained using the set of quantiles. It looks like the optimal threshold for binary classification of severe car crashes is given by the 0.975-quantile, where the balanced accuracy distribution is

⁸We decided to adopt one as a threshold to dichotomise the variables since more than 80% of road segments registered no severe car crash during 2011-2018. The procedure proposed here can be extended to three or more classes, defined using a set of different thresholds (such as *Zero*, *One*, and *Two or more* road crashes).

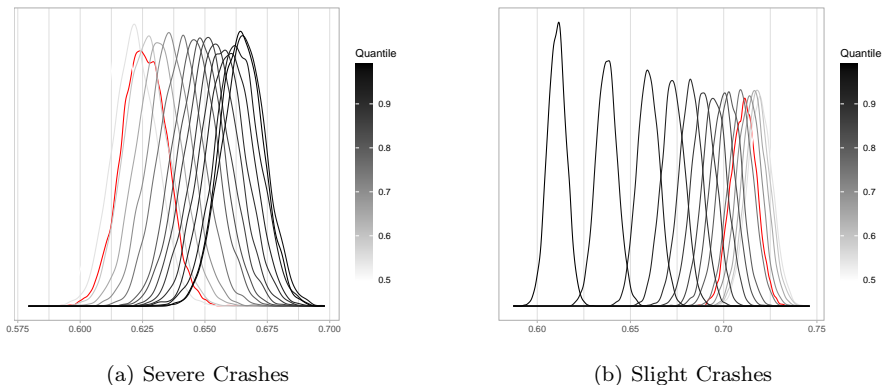


Figure 6: Distribution of balanced accuracy for severe crashes (right) and slight crashes (left), considering a binary classification using the posterior mean and a set of quantiles. The red curve represents the mean.

concentrated around 0.66. The optimal threshold for binary classification of slight car crashes is given by the median, and the distribution of balanced accuracy is centred around 0.72. These plots remark the differences between the two severity levels in terms of sparsity, suggesting the adoption of a higher quantile for the prediction of the more sparse events. However, using the appropriate cut-off(s), Model (G) seems to perform reasonably well in both cases with slightly better performance for slight car crashes.

5.2 Second strategy for criticism

Following the results illustrated before, we estimated the 0.975-quantile of λ_{i1} (severe crashes) and the median of λ_{i2} (slight crashes), and we multiplied them by the corresponding offset values, i.e. E_i . Then, we created a sequence of histograms of predicted values, grouped by the observed counts categorised in four levels: 0, 1, 2, and 3 or more. The results are summarised in Figure 7a and Figure 7b. Both graphs show a good agreement between predicted and observed number of crashes, since the distributions corresponding to higher observed counts progressively move more and more to the right. Moreover, Figure 7a shows the importance of our previous analysis and the pitfalls of predicting severe car crashes counts using the posterior means.

5.3 Sensitivity analysis and the modifiable areal unit problem

Finally, we performed a sensitivity analysis evaluating the robustness of model (G) under different specifications for 1) the hyperprior distributions, 2) the adjacency matrix, and 3) the definition of the segments in the road network.

The models described in Section 3 considered a Wishart hyperprior for precision matrix Ω with rank equal to 2 and scale matrix equal to \mathbf{I}_2 . We repeated the analysis using more vague and more informative Wishart distributions, setting the scale matrix equal to $\text{diag}(2, 2)$ and $\text{diag}(0.5, 0.5)$. We did not find any noticeable differences amongst alternative specifications. Hence results are not reported hereafter, but we refer the interested readers to the supplementary material.

We compared different definitions for the adjacency matrix \mathbf{W} , testing second and

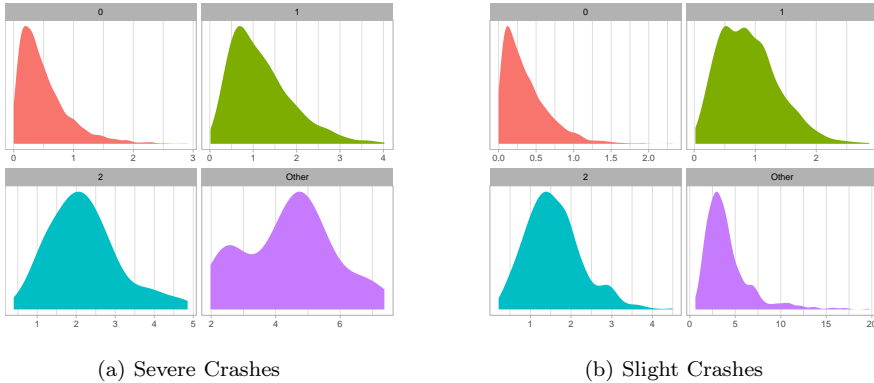


Figure 7: Histogram of posterior 0.975-quantile (left) and posterior median (right), grouped by the corresponding observed counts. Other means "Three or more."

third order neighbours and distance-based spatial neighbours⁹. Also in this case, we did not find any noticeable differences as far as the estimation of the fixed effects is concerned, whereas only small differences were found in the posterior distributions of the random effects (especially for $\sigma_{\phi_1}^2$ and $\sigma_{\phi_2}^2$ when we considered a spatial adjacency matrix with a threshold equal to $500m$). However, worse DIC and wAIC values were found for models using alternative definitions of \mathbf{W} matrix, and we refer to the supplementary material for more details. Similar findings are also reported by [2, 66] and [4].

Finally, we explored the influence of a particular configuration of the network segments on our results. In fact, the location of the vertices (and, hence, the edges) in a road network created with OS data is essentially arbitrary (although some minimal consistency requirements must be satisfied, see [25, 29]), which implies that there is no unique and unambiguous way of defining the lengths and relative positions of the road segments. We, therefore, considered an alternative network configuration reshaping and contracting the road network using an algorithm implemented in [51]. This algorithm manipulates a network by excluding all *redundant* vertices, i.e. those vertices that connect two contiguous segments without any other intersection [51].

A toy example representing the ideas behind the contraction of a road network is sketched in Figure 8. The red dots in Figure 8a represent redundant vertices since they can be removed without tampering the shape or the routability of the network¹⁰. The goal is to remove all redundant vertices and merge the corresponding edges, creating a graph which looks identical to the original one but with fewer edges. Figure 8b shows the results of the contraction operations applied to the toy network sketched in Figure 8a. We can see that the redundant vertices were removed, combining the road segments that touched them.

Applying this algorithm produced a contracted road network with, approximately, 2700 segments (instead of the original 3661). Following the same procedures detailed in Sections 2 and 4, we calculated the number of severe and slight car crashes that

⁹In this case two road segments are considered neighbours if the euclidean distance between their centroids is smaller than a certain threshold. In particular, we used $25m$, $50m$, $100m$, $250m$ and $500m$ as alternative thresholds. In case a network segment was longer than twice the threshold, we consider first order neighbours to avoid the creation of several islands (see Section 2). This problem is more pronounced for smaller values of the threshold.

¹⁰We say that the algorithm in [51] preserves the *routability* of a road network since it does not remove any vertex that could add a new *component* to the graph.

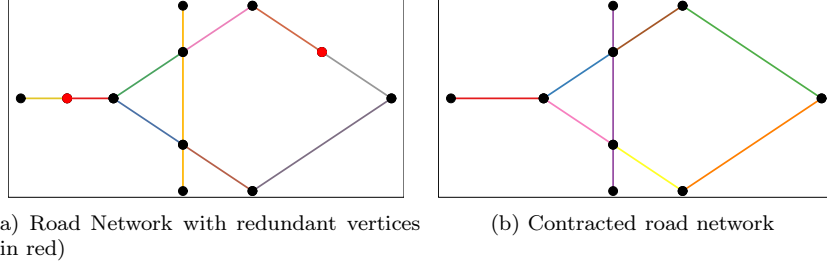


Figure 8: Sketching of the algorithm used for contracting the road network. Red points on the left represent redundant vertices.

	Severe Crashes	Slight Crashes
β_0	-15.335 (0.233)	-13.694 (0.198)
Betweenness	-0.008 (0.055)	-0.041 (0.037)
Motorways	-0.872 (0.180)	-0.298 (0.140)
Primary Roads	0.413 (0.132)	0.496 (0.117)

Table 6: Means and standard deviations for the posterior distributions of the fixed effects in the model estimated after contracting the road network.

	$\sigma_{\theta_1}^2$	$\sigma_{\theta_2}^2$	ρ_θ	ρ_1	ρ_2	$\sigma_{\phi_1}^2$	$\sigma_{\phi_2}^2$	ρ_ϕ
mean:	0.307	0.500	0.388	0.995	0.993	3.970	4.767	0.944
sd:	(0.103)	(0.100)	(0.020)	(0.003)	(0.003)	(0.630)	(0.622)	(0.016)

Table 7: Means and standard deviations for the posterior distributions of the hyperparameters in the model estimated after contracting the road network.

occurred in each road segment, the traffic volumes (which are used as an offset), and the edge betweenness centrality measures. The road type was automatically determined since the algorithm did not merge two road segments with different classifications. Finally, we estimated model (G) and reported a summary of means and standard errors of the posterior distributions of fixed and random effects in Tables 6 and 7, respectively.

As far as the fixed effects are concerned, the new network configuration influences results quite mildly, since the estimates of the coefficients did not change in sign, order of magnitude or significance. As one could expect, the impact of network reshaping is slightly more pronounced for the random effects, in particular for $\sigma_{\phi_1}^2$ and $\sigma_{\phi_2}^2$, two of the five hyperparameters in the PMCAR prior. The model trained on the contracted network presents a greater spatial uncertainty than model (G), but similar posterior distributions for car crashes rates. We refer the interested readers to the supplementary material, where we also reported the maps of predicted rates using the new network configuration.

Network reshaping and contraction is a network-readaptation of the classical Modifiable Area Unit Problem (MAUP), only recently explored by a handful of authors in the literature of road safety models for areal data (see, for example, [69] for an introduction, and [15] for an extensive application). The main conclusion of these papers is that MAUP severely impacts car crashes models, affecting the magnitude and significance of the estimates for both fixed and random effects, hence it should never be ignored for a reliable road safety analysis.

Our results tell a somewhat different story. The statistical analysis is found quite robust to MAUP when carried out on a network lattice, possibly because the road network has a physical geometrical meaning and, hence, a lower degree of arbitrariness than administrative boundaries. Hence, we suggest not to ignore the network structure of the data whenever it is available when analysing car crashes data or other phenomena that naturally occur on a network. The only paper that performs a descriptive analysis of the influence of road segment configurations on car crashes counts is [60], and, to the best of our knowledge, this is the first attempt to explore the robustness of a statistical model for lattice network data to MAUP.

6 Conclusions

This paper investigated the spatial distribution of road crashes in a major city using new methods for network analysis. The relationship between crashes of different severity levels, either *slight* or *severe*, were modelled using a range of multivariate models to explore their spatial dynamics. Key to the approach was constraining crash locations to the city’s road network, a one-dimensional linear network composed of segments representing a spatial lattice.

We found that the best model includes a multivariate spatially unstructured random effect and a multivariate spatially structured PMCAR random effect with a different autocorrelation parameter for each severity level. The results, which are summarised in Tables 2 and 3, suggest that the Motorways are less prone to severe and slight car crashes than A-roads, which are also less dangerous than Primary roads. The posterior distributions of the hyperparameters point out a strong between-level correlation in the unstructured errors and an even stronger dependence in the spatial component.

The approach proposed in this paper allows the estimation of a severity specific car crashes rate for every single segment in the road network, which can be visualised using an appropriate choropleth map. Figure 5 exemplifies this process by showing two maps that display the posterior means of car crash rates for severe and slight accidents. They highlight several roads, or portions of a road, mainly located in the north-east, north-west and south-east of Leeds city centre, which are associated with higher car crashes rates. The two maps illustrate that adopting a network-based approach allows the identification of dangerous streets more precisely than using an areal-based aggregation. These results could represent the starting point for further analysis, linking car crashes rates with structural aspects of the network such as roundabouts, street junctions or pedestrian crossings, hence, in turn, identifying and evaluating potential levers to intervene on. This extension was ignored in the current paper since it requires a different methodological approach, and OS data do not include a precise database of roundabouts or street junctions.

We evaluated the sensitivity of our modelling approach to different hyperprior specifications and adjacency configurations of the components of the lattice network, showing that the statistical model presents substantial robustness in this respect. We finally considered the impact of MAUP when modelling data collected on a spatial network. An algorithm was proposed in the paper to assess the magnitude of MAUP effect in the estimates and model predictions.

Differently from several previous studies that considered the MAUP for various areal partitions of the spatial region of interest, we found that our results are quite robust under an alternative configuration of the road network. This can be related to the fact that road networks have a physical meaning, hence they are expected to suffer MAUP less, a further advantage of the network approach. Robustness of results is fundamental for the development of a reliable model that can be used to support the implementation of new policies. Nevertheless, further research, possibly in different fields, is definitely necessary to better understand the impact of MAUP on network lattice data.

The ideas presented in this paper could be extended in several directions. A first step forward could be focused towards the development of a spatio-temporal extension of model (G), following the suggestions in [44, 65, 12, 36]. We point out, however, that this is not straightforward (and, to the best of our knowledge, it was pursued only by [36] using a single road divided into a few segments) given the extreme sparse spatio-temporal nature of severe car crashes on a metropolitan road network. Indeed, for the dataset at hand, more than 95% of all car crashes registered no fatal or serious car accident for any given year, something that could require a different methodological approach. The procedure for MAUP detection could also be improved by developing new routines for testing alternative algorithms for network reshaping and contraction, which were first developed for areal data in the field of geography (see, e.g., [69] and references therein). An additional improvement to the approach could involve the development of spatial or spatio-temporal theoretical point pattern models for car crashes on networks. It is clear that more research is needed to evaluate the full range of possible models for identifying crash ‘hot spots’ on the network. The research presented in this paper demonstrates the potential of network-based approaches to work at city scales for flexible and robust estimates of crash rates, down to the road segment level and provides a basis for more further work in the field.

Acknowledgement

Contains OS data © Crown copyright [and database right] 2020. J. Mateu is partially supported by funds PID2019-107392RB-I00 and AICO/2019/198. We greatly acknowledge the DEMS Data Science Lab for supporting this work by providing computational resources.

References

- [1] Mohamed Abdel-Aty et al. “Geographical unit based analysis in the context of transportation safety planning”. In: *Transportation Research Part A: Policy and Practice* 49 (2013), pp. 62–75.
- [2] Jonathan Aguero-Valverde and Paul P Jovanis. “Analysis of Road Crash Frequency with Spatial Models”. In: *Transportation Research Record* 2061.1 (2008), pp. 55–63. DOI: 10.3141/2061-07. eprint: <https://doi.org/10.3141/2061-07>. URL: <https://doi.org/10.3141/2061-07>.
- [3] Jonathan Aguero-Valverde and Paul P Jovanis. “Spatial analysis of fatal and injury crashes in Pennsylvania”. In: *Accident Analysis & Prevention* 38.3 (2006), pp. 618–625.
- [4] Saif A Alarifi et al. “Exploring the effect of different neighboring structures on spatial hierarchical joint crash frequency models”. In: *Transportation Research Record* 2672.38 (2018), pp. 210–222.

- [5] Adrian Baddeley et al. “Analysing point patterns on networks—A review”. In: *Spatial Statistics* (2020), p. 100435.
- [6] Sudip Barua, Karim El-Basyouny, and Md Tazul Islam. “A full Bayesian multivariate count data model of collision severity with spatial correlation”. In: *Analytic Methods in Accident Research* 3 (2014), pp. 28–43.
- [7] Karim El-Basyouny and Tarek Sayed. “Urban arterial accident prediction models with spatial effects”. In: *Transportation Research Record* 2102.1 (2009), pp. 27–33.
- [8] Julian Besag. “Spatial interaction and the statistical analysis of lattice systems”. In: *Journal of the Royal Statistical Society: Series B (Methodological)* 36.2 (1974), pp. 192–225.
- [9] Julian Besag and Charles Kooperberg. “On conditional and intrinsic autoregressions”. In: *Biometrika* 82.4 (1995), pp. 733–746.
- [10] Riccardo Borgoni, Andrea Gilardi, and Diego Zappa. “Assessing the Risk of Car Crashes in Road Networks”. In: *Social Indicators Research* (2020), pp. 1–19.
- [11] P Botella-Rocamora, A Lopez-Quilez, and MA Martinez-Beneito. “Spatial moving average risk smoothing”. In: *Statistics in Medicine* 32.15 (2013), pp. 2595–2612.
- [12] Areti Boulieri et al. “A space–time multivariate Bayesian model to analyse road traffic accidents by severity”. In: *Journal of the Royal Statistical Society: Series A (Statistics in Society)* 180.1 (2017), pp. 119–139.
- [13] David Braunholtz and Duncan Elliott. *Estimating and adjusting for changes in the method of severity reporting for road accidents and casualty data*. Available at: https://assets.publishing.service.gov.uk/government/uploads/system/uploads/attachment_data/file/414444/Estimating_and_adjusting_for_changes_in_the_method_of_severity_reporting_for_road_accidents_and_casualty_data.pdf. Department for Transport. 2019.
- [14] Álvaro Briz-Redón, Francisco Martínez-Ruiz, and Francisco Montes. “Estimating the occurrence of traffic accidents near school locations: a case study from Valencia (Spain) including several approaches”. In: *Accident Analysis & Prevention* 132 (2019), p. 105237.
- [15] Álvaro Briz-Redón, Francisco Martínez-Ruiz, and Francisco Montes. “Investigation of the consequences of the modifiable areal unit problem in macroscopic traffic safety analysis: a case study accounting for scale and zoning”. In: *Accident Analysis & Prevention* 132 (2019), p. 105276.
- [16] K. H. Brodersen et al. “The Balanced Accuracy and Its Posterior Distribution”. In: *2010 20th International Conference on Pattern Recognition*. 2010, pp. 3121–3124.
- [17] Bradley P Carlin, Sudipto Banerjee, et al. “Hierarchical multivariate CAR models for spatio-temporally correlated survival data”. In: *Bayesian Statistics* 7.7 (2003), pp. 45–63.
- [18] Noel AC Cressie. *Statistics for Spatial Data*. John Wiley & Sons, Ltd, 1993.
- [19] Ottmar Cronie, Mehdi Moradi, and Jorge Mateu. “Inhomogeneous higher-order summary statistics for point processes on linear networks”. In: *Statistics and Computing* (2020).

- [20] Department for Transport. *Reported road casualties in Great Britain: 2019 annual report*. Available at: https://assets.publishing.service.gov.uk/government/uploads/system/uploads/attachment_data/file/871222/road-casualties-2019-annual-report.pdf. 2020.
- [21] Robin A Dubin. “Estimation of regression coefficients in the presence of spatially autocorrelated error terms”. In: *The Review of Economics and Statistics* (1988), pp. 466–474.
- [22] Anna Freni-Sterrantino, Massimo Ventrucci, and Håvard Rue. “A note on intrinsic conditional autoregressive models for disconnected graphs”. In: *Spatial and Spatio-temporal Epidemiology* 26 (2018), pp. 25–34. ISSN: 1877-5845. DOI: <https://doi.org/10.1016/j.sste.2018.04.002>. URL: <http://www.sciencedirect.com/science/article/pii/S1877584517301600>.
- [23] Alan E Gelfand and Penelope Vounatsou. “Proper multivariate conditional autoregressive models for spatial data analysis”. In: *Biostatistics* 4.1 (2003), pp. 11–15.
- [24] Andrew Gelman, Jessica Hwang, and Aki Vehtari. “Understanding predictive information criteria for Bayesian models”. In: *Statistics and Computing* 24.6 (2014), pp. 997–1016.
- [25] Andrea Gilardi, Robin Lovelace, and Mark Padgham. *Street Networks in R*. Sept. 2020. URL: osf.io/78yub.
- [26] Virgilio Gómez-Rubio. *Bayesian Inference with INLA*. CRC Press, 2020.
- [27] Leonhard Held, Birgit Schrödle, and Håvard Rue. “Posterior and cross-validatory predictive checks: a comparison of MCMC and INLA”. In: *Statistical modelling and regression structures*. Springer, 2010, pp. 91–110.
- [28] James S Hodges, Bradley P Carlin, and Qiao Fan. “On the precision of the conditionally autoregressive prior in spatial models”. In: *Biometrics* 59.2 (2003), pp. 317–322.
- [29] Alireza Karduni, Amirhassan Kermanshah, and Sybil Derrible. “A protocol to convert spatial polyline data to network formats and applications to world urban road networks”. In: *Scientific Data* 3.1 (2016), pp. 1–7.
- [30] David S. Kirk, Nicolo Cavalli, and Noli Brazil. “The Implications of Ride-hailing for Risky Driving and Road Accident Injuries and Fatalities”. en. In: *Social Science & Medicine* 250 (Apr. 2020), p. 112793. ISSN: 0277-9536. DOI: [10.1016/j.socscimed.2020.112793](https://doi.org/10.1016/j.socscimed.2020.112793).
- [31] Eric D Kolaczyk and Gábor Csárdi. *Statistical analysis of network data with R*. Vol. 65. Springer, 2014.
- [32] Finn Lindgren and Håvard Rue. “Bayesian Spatial Modelling with R-INLA”. In: *Journal of Statistical Software* 63.19 (2015), pp. 1–25. URL: <http://www.jstatsoft.org/v63/i19/>.
- [33] Dominique Lord and Fred Mannering. “The statistical analysis of crash-frequency data: a review and assessment of methodological alternatives”. In: *Transportation research part A: policy and practice* 44.5 (2010), pp. 291–305.
- [34] Robin Lovelace and Layik Hama. *pct: Propensity to Cycle Tool*. R package version 0.4.0. 2020. URL: <https://CRAN.R-project.org/package=pct>.

- [35] Robin Lovelace et al. “stats 19: A package for working with open road crash data”. In: *The Journal of Open Source Software* 4.33 (Jan. 2019), p. 1181. DOI: 10.21105/joss.01181.
- [36] Xiaoxiang Ma, Suren Chen, and Feng Chen. “Multivariate space-time modeling of crash frequencies by injury severity levels”. In: *Analytic Methods in Accident Research* 15 (2017), pp. 29–40.
- [37] Murray MacKay. “Traffic Accidents—a Modern Epidemic”. In: *International Journal of Environmental Studies* 3.1-4 (Jan. 1972), pp. 223–227. ISSN: 0020-7233. DOI: 10.1080/00207237208709519.
- [38] KV Mardia. “Multi-dimensional multivariate Gaussian Markov random fields with application to image processing”. In: *Journal of Multivariate Analysis* 24.2 (1988), pp. 265–284.
- [39] EC Marshall and DJ Spiegelhalter. “Approximate cross-validators predictive checks in disease mapping models”. In: *Statistics in Medicine* 22.10 (2003), pp. 1649–1660.
- [40] Stephen Marshall et al. “Street network studies: from networks to models and their representations”. In: *Networks and Spatial Economics* 18.3 (2018), pp. 735–749.
- [41] Miguel A Martínez-Beneito and Paloma Botella-Rocamora. *Disease Mapping: From Foundations to Multidimensional Modeling*. CRC Press, 2019.
- [42] Shaw-Pin Miaou. “The relationship between truck accidents and geometric design of road sections: Poisson versus negative binomial regressions”. In: *Accident Analysis & Prevention* 26.4 (1994), pp. 471–482.
- [43] Shaw-Pin Miaou and Harry Lum. “Modeling vehicle accidents and highway geometric design relationships”. In: *Accident Analysis & Prevention* 25.6 (1993), pp. 689–709.
- [44] Shaw-Pin Miaou and Joon Jin Song. “Bayesian ranking of sites for engineering safety improvements: decision parameter, treatability concept, statistical criterion, and spatial dependence”. In: *Accident Analysis & Prevention* 37.4 (2005), pp. 699–720.
- [45] Shaw-Pin Miaou, Joon Jin Song, and Bani K Mallick. “Roadway traffic crash mapping: a space-time modeling approach”. In: *Journal of transportation and Statistics* 6 (2003), pp. 33–58.
- [46] Vinand M Nantulya and Michael R Reich. “The Neglected Epidemic: Road Traffic Injuries in Developing Countries”. In: *BMJ : British Medical Journal* 324.7346 (May 2002), pp. 1139–1141. ISSN: 0959-8138.
- [47] Robert B Noland and Mohammed A Quddus. “A spatially disaggregate analysis of road casualties in England”. In: *Accident Analysis & Prevention* 36.6 (2004), pp. 973–984.
- [48] Stan Openshaw. “The modifiable areal unit problem”. In: *Quantitative Geography: A British view* (1981), pp. 60–69.
- [49] Ordnance Survey. *Ordnance Survey*. Accessed: 2020-05-21. 2020. URL: <https://www.ordnancesurvey.com>
- [50] PACTS. *Roads Policing and Its Contribution to Road Safety*. Tech. rep. Parliamentary Advisory Council for Transport Safety, 2020.

- [51] Mark Padgham. “dodgr: An R package for network flow aggregation”. In: *Transport Findings* (Feb. 2019). DOI: 10.32866/6945.
- [52] Francisco Palmi-Perales, Virgilio Gomez-Rubio, and Miguel A. Martinez-Beneito. *Bayesian Multivariate Spatial Models for Lattice Data with INLA*. 2019. arXiv: 1909.10804 [stat.CO].
- [53] Sergio Porta, Paolo Crucitti, and Vito Latora. “The network analysis of urban streets: a dual approach”. In: *Physica A: Statistical Mechanics and its Applications* 369.2 (2006), pp. 853–866.
- [54] R Core Team. *R: A Language and Environment for Statistical Computing*. R Foundation for Statistical Computing, Vienna, Austria, 2020. URL: <https://www.R-project.org/>.
- [55] Suman Rakshit et al. “Fast Kernel Smoothing of Point Patterns on a Large Network using Two-dimensional Convolution”. In: *International Statistical Review* 87.3 (2019), pp. 531–556.
- [56] Håvard Rue et al. “Bayesian computing with INLA: A review”. In: *Annual Reviews of Statistics and Its Applications* 4.March (2017), pp. 395–421. URL: <http://arxiv.org/abs/1604.00860>.
- [57] Peter T Savolainen et al. “The statistical analysis of highway crash-injury severities: a review and assessment of methodological alternatives”. In: *Accident Analysis & Prevention* 43.5 (2011), pp. 1666–1676.
- [58] Venkataraman Shankar, Fred Mannering, and Woodrow Barfield. “Effect of roadway geometrics and environmental factors on rural freeway accident frequencies”. In: *Accident Analysis & Prevention* 27.3 (1995), pp. 371–389.
- [59] David J Spiegelhalter et al. “Bayesian measures of model complexity and fit”. In: *Journal of the Royal Statistical Society: Series B (Statistical Methodology)* 64.4 (2002), pp. 583–639.
- [60] Isabelle Thomas. “Spatial data aggregation: exploratory analysis of road accidents”. In: *Accident Analysis & Prevention* 28.2 (1996), pp. 251–264.
- [61] UK Data Service Census Support. *Census Support: Flow Data*. 2014. URL: <http://wicid.ukdataservice.ac.uk/>.
- [62] Satish Ukkusuri et al. “The role of built environment on pedestrian crash frequency”. In: *Safety Science* 50.4 (2012), pp. 1141–1151.
- [63] Melanie M Wall. “A close look at the spatial structure implied by the CAR and SAR models”. In: *Journal of Statistical Planning and Inference* 121.2 (2004), pp. 311–324.
- [64] Chao Wang, Mohammed A Quddus, and Stephen G Ison. “Impact of traffic congestion on road accidents: a spatial analysis of the M25 motorway in England”. In: *Accident Analysis & Prevention* 41.4 (2009), pp. 798–808.
- [65] Chao Wang, Mohammed A Quddus, and Stephen G Ison. “Predicting accident frequency at their severity levels and its application in site ranking using a two-stage mixed multivariate model”. In: *Accident Analysis & Prevention* 43.6 (2011), pp. 1979–1990.
- [66] Xuesong Wang et al. “Macro-level safety analysis of pedestrian crashes in Shanghai, China”. In: *Accident Analysis & Prevention* 96 (2016), pp. 12–21.

- [67] Sumio Watanabe. “Asymptotic Equivalence of Bayes Cross Validation and Widely Applicable Information Criterion in Singular Learning Theory”. In: *Journal of Machine Learning Research* 11 (2010), pp. 3571–3594.
- [68] World Health Organization. *Global Status Report On Road Safety 2018*. en. World Health Organization, 2018. ISBN: 978-92-4-156568-4.
- [69] Pengpeng Xu, Helai Huang, and Ni Dong. “The modifiable areal unit problem in traffic safety: basic issue, potential solutions and future research”. In: *Journal of Traffic and Transportation Engineering (English edition)* 5.1 (2018), pp. 73–82.
- [70] Xiaoqi Zhai et al. “The influence of zonal configurations on macro-level crash modeling”. In: *Transportmetrica A: transport science* 15.2 (2019), pp. 417–434.
- [71] Apostolos Ziakopoulos and George Yannis. “A review of spatial approaches in road safety”. In: *Accident Analysis & Prevention* 135 (2020), p. 105323.